THE JOURNAL OF PHYSICAL CHEMISTRY B LETTERS

2005, *109,* 6968−6971
Published on Web 03/24/2005

On the Origin of Preferential Growth of Semiconducting Single-Walled Carbon Nanotubes

Yiming Li,[†] Shu Peng,[‡] David Mann,[†] Jien Cao,[†] Ryan Tu,[†] K. J. Cho,[‡] and Hongjie Dai*[,†]

Department of Chemistry and Laboratory for Advanced Materials, Stanford University, Stanford, California 94305, and Department of Mechanical Engineering, Stanford University, Stanford, California 94305

Received: February 19, 2005

A correlation is observed between the diameters (d) of single-walled carbon nanotubes and the percentages of metallic and semiconducting tubes synthesized at 600 °C by plasma-assisted chemical vapor deposition. Small tubes ($d \approx 1.1$ nm) show semiconductor percentages that are much higher than expected for a random chirality distribution. Density functional theory calculations reveal differences in the heat of formation energies for similar-diameter metallic, quasi-metallic, and semiconducting nanotubes. Semiconducting tubes exhibit the lowest energies and the stabilization scales with $\sim 1/d^2$. This could be a thermodynamic factor in the preferential growth of small semiconducting nanotubes.

The chirality of a single-walled carbon nanotube (SWNT) determines whether the nanotube is a metal or semiconductor.[1] Although semiconducting SWNTs (S-SWNTs) can be used to build high-performance field-effect transistors and sensors,[2−4] metallic SWNTs (M-SWNTs) might be useful for interconnects. However, these potential applications clearly will hinge on obtaining purely metallic and semiconducting nanotubes.[5] One approach might be chemically separating metallic from semiconducting SWNTs,[6−10] and another could be via selective growth to produce a certain type of nanotubes preferentially.[11] Recently, we reported a plasma-enhanced chemical vapor deposition (PECVD) method that produced SWNTs at 600 °C with the percentage of S-SWNTs being ~89%.[11] In other work, using materials synthesized by a thermal chemical vapor deposition (CVD) method, Bachilo et al. even observed that SWNTs with certain chiralities were formed preferentially.[12] It seems that selective growth of certain types of nanotubes can indeed occur. However, little is known thus far about the driving forces behind the preferential growth phenomena.

Here, we report that higher percentages of S-SWNTs are grown when the growth parameters are adjusted to produce smaller-diameter SWNTs at a relatively low growth temperature of 600 °C. First-principles calculations reveal that SWNTs of different metallicity exhibit discernible differences in the heat of formation energies. S-SWNTs show the lowest energies and are the most stable, compared to metallic and quasi-metallic[13] SWNTs (QM-SWNT with band gaps of approximately tens of meV). This could be a factor that leads to the preferential growth of semiconducting nanotubes.

We performed the synthesis of SWNTs in a 4-in. quasi-remote PECVD system (radio frequency (RF), 13.56 MHz) at 600 °C using discrete ferritin nanoparticles[14] as catalysts on SiO_2/Si substrates (SiO_2 thickness of $t_{ox} = 67$ nm), as described previously.[11] The methane flow rate was 60 sccm (sccm ≡ standard cubic centimeters per minute), and the pressure in the PECVD system was maintained at 500 mTorr. The plasma power was varied over a range of 50−200 W, and the growth time was typically 3 min.

We found that, at a fixed growth temperature of 600 °C, varying the plasma power over a range of 50−200 W led to an obvious shift in the diameter distribution of the synthesized nanotubes. Atomic force microscopy (AFM) imaging (Figure 1a, 1b) and topographic measurements (Figure 1c, 1d) revealed the mean diameters of nanotubes produced by 50-W and 200-W PECVD are $\langle d \rangle = 1.12 \pm 0.25$ nm and $\langle d \rangle = 1.66 \pm 0.38$ nm, respectively. More than 80% of the nanotubes in the 50-W sample (referenced herein as sample A) had mean diameters of $d < 1.4$ nm (see Figure 1e), whereas most (~76%) nanotubes in the 200-W sample (referenced herein as sample B) exhibited mean diameters of $d > 1.4$ nm (see Figure 1f). Note that the catalysts used for samples A and B were the same, with diameters in the range of 0.7−3 nm. Under the otherwise identical growth conditions, higher plasma power apparently allowed for the growth of larger-diameter SWNTs from larger particles, as evidenced by the clear shift in the SWNT diameter distribution. We attribute this to more-effective decomposition of methane at higher plasma power, providing more-efficient carbon feedstock, which is needed for the supersaturation of larger catalyst particles and, thus, the growth of larger tubes.

With the synthesized nanotubes on SiO_2/Si substrates, we fabricated large arrays of three-terminal devices, each comprised of a Pd[3] source (S), a drain (D), a back-Si-gate, and one or multiple SWNTs bridging S/D (Figure 2a, inset). We then used electrical transport measurements to assess whether the SWNTs are metallic or semiconducting.[11] Devices comprised of only S-SWNTs exhibited conductance changes of several orders of magnitude (termed "depletable") under electrostatic gating (see Figure 2a), whereas devices comprised of M- and/or QM-SWNTs exhibit weak gate dependence (termed "nondepletable" for both M- and QM-SWNTs). We used an electrical breakdown

* Author to whom correspondence should be addressed. E-mail address: hdai@stanford.edu.
[†] Department of Chemistry and Laboratory for Advanced Materials.
[‡] Department of Mechanical Engineering.

10.1021/jp050868h CCC: $30.25

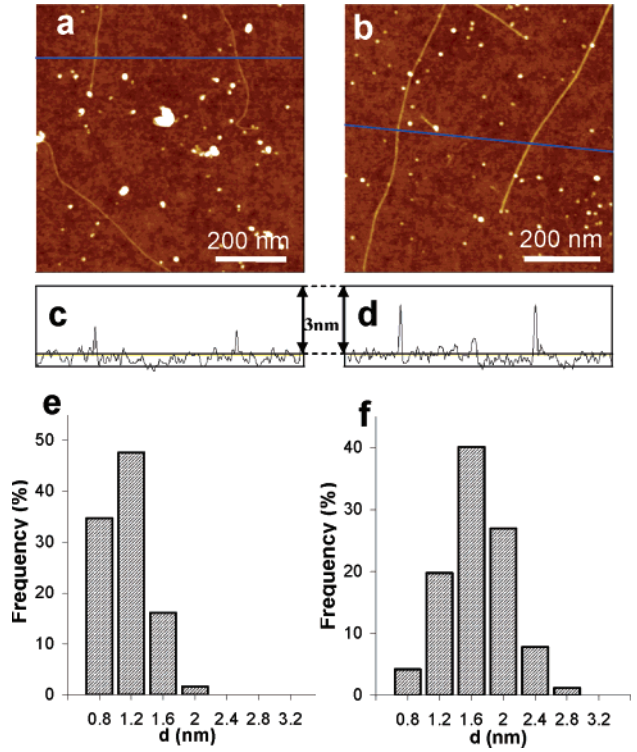

Figure 1. Atomic force microscopy (AFM) images of nanotubes grown by plasma-enhanced chemical vapor deposition (PECVD) under a plasma power of (a) 50 W (sample A) and (b) 200 W (sample B). (c and d) Corresponding topographic height profiles along the dark lines drawn in panels a and b, respectively. (e) Diameter distribution for sample A, obtained over 124 tubes. (f) Diameter distribution for sample B, obtained over 167 tubes. Note that the diameter distributions measured by the Raman shifts of radial breathing modes detailed in ref 11 were consistent with the AFM results shown here.

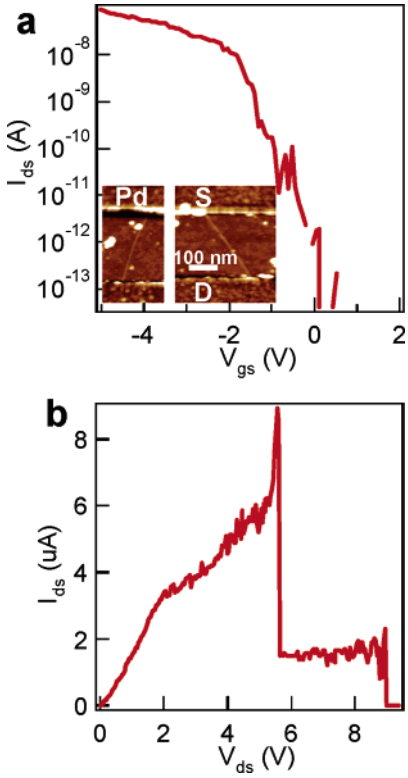

Figure 2. (a) Plot of current (I_{ds}) versus gate voltage (V_g) (recorded under a bias of $V_{ds} = 100$ mV) for a two-tube semiconducting device (see inset), showing 10^6 *p*-channel conductance depletion by sweeping the gate. Inset shows an AFM image of two nanotubes ($d \approx 1.2$ and 1.3 nm, respectively) bridging palladium S/D electrodes in a device (with a channel length of $L \approx 300$ nm). (b) I_{ds} vs V_{ds} curve recorded under $V_g = -5$ V (both tubes in the ON-state), showing sequential electrical breakdown of the two tubes in the device.

method (see Figure 2b) that was detailed previously[11] to "count" larger numbers of M-/QM-SWNTs and S-SWNTs in each device. Using this method, we identified ~86% (±3%) and ~75% (±4%) S-SWNTs in sample A (the number of tubes analyzed was $N_T = 386$) and sample B ($N_T = 335$), respectively. The former was similar to that of ~89% S-SWNTs in samples synthesized under similar plasma power. These results reveal preferential growth of S-SWNTs in small-diameter ($\langle d \rangle \approx 1.1$ nm) samples and reduced percentages of S-SWNTs in the larger-diameter samples ($\langle d \rangle \approx 1.7$ nm).

Figure 3a and 3b summarize the maximum device conductance (G_{max}, measured over the experimentally accessible gate-voltage range) measured with over 100 devices for samples A and B, respectively. We observe that the depletable devices (comprised of only S-SWNTs) generally exhibit lower G_{max} values than the nondepletable devices bridged by M- or QM-SWNTs. This is attributed to differences in junction resistance that are due to the existence of Schottky barriers (SBs) at the metal/S-SWNT contacts and no significant SBs at the contacts for M/QM-SWNTs. Large numbers of the depletable devices in sample B (see Figure 3b) exhibit higher G_{max} values than those in sample A (see Figure 3a), corresponding to the larger-diameter S-SWNTs in sample B, affording lower SBs at the palladium contacts, because of smaller band gaps ($E_{gap} \approx 1/d$) and, thus, higher ON-conductance.[3] Importantly, for both samples A and B, devices with lower G_{max} values (i.e., comprised of smaller-diameter tubes) clearly show higher percentages of depletable devices than nondepletable ones. This can be gleaned from Figure 3, in that the ratio between light (percentage of depletable devices) and dark (nondepletable devices) bars in each G_{max} range has a tendency to be larger for smaller G_{max} values or smaller-diameter tubes. This again suggests higher percentages of S-SWNTs for tubes with smaller diameters.

To understand the origin of preferential formation of S-SWNTs, we conducted density functional theory (DFT) calculations to investigate the energetics and stability of various types of nanotubes. Self-consistent electronic structure calculations were performed using the ultra-soft pseudo-potential code VASP[15] with local density approximation (LDA) at a kinetic energy cutoff of 21 Rydberg. Supercells that contain one-unit cells of nanotubes (the number of C atoms in a unit cell is dependent on diameter and chirality and can be up to 196) were used. The Brillouin zone sampling was approximated by 12 k-points along the tube axis. Electronic minimization was performed to a convergence tolerance of 0.1 meV, and the structures were relaxed until the maximum forces on any C atom was <0.015 eV/Å. The cohesive energy and heat of formation of SWNT per C atom is defined as

$$\Delta H = \frac{E_{\text{total}}(\text{SWNT})}{\text{number of atoms}} - E(\text{C}) \qquad (1)$$

where E(C) is the energy for an isolated C atom. The atomic heats of formation for various M-, QM-, and SWNTs with diameters in the range of $d = 1-2$ nm, together with that of a flat graphene, are plotted in Figure 4a. The heat of formation for the three types of tubes, relative to that of graphene, can be well fit into $\sim 1/d^2$ forms (solid lines in Figure 4a). Importantly, for a given value of d, we consistently find that S-SWNTs

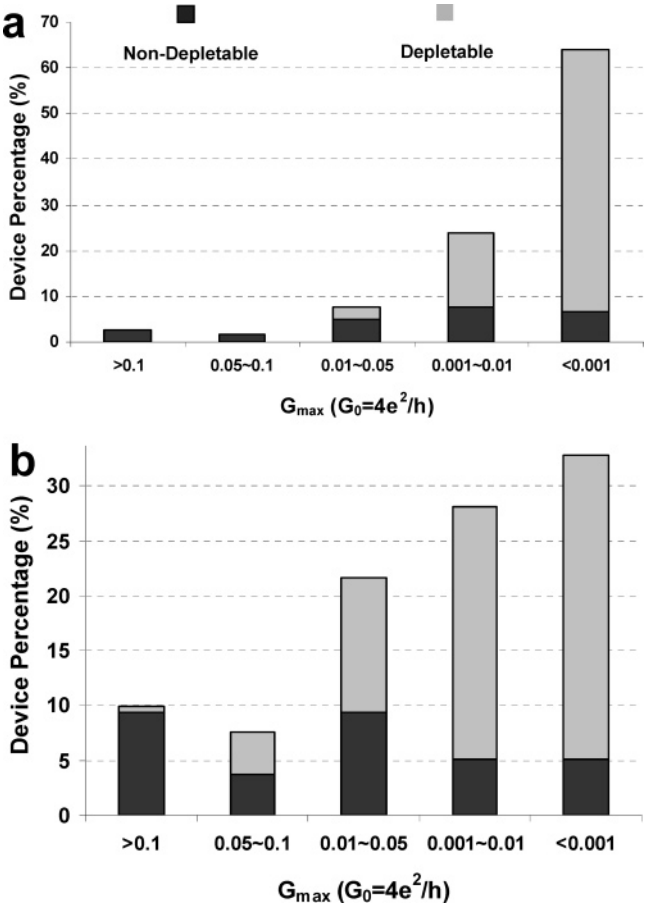

Figure 3. Graphs showing the percentages of depletable and non-depletable devices with G_{max} (i.e., maximum conductance measured in the gate-voltage range of −5 to 5 V) in various ranges (noted along the *x*-axis): (a) sample A and (b) sample B.

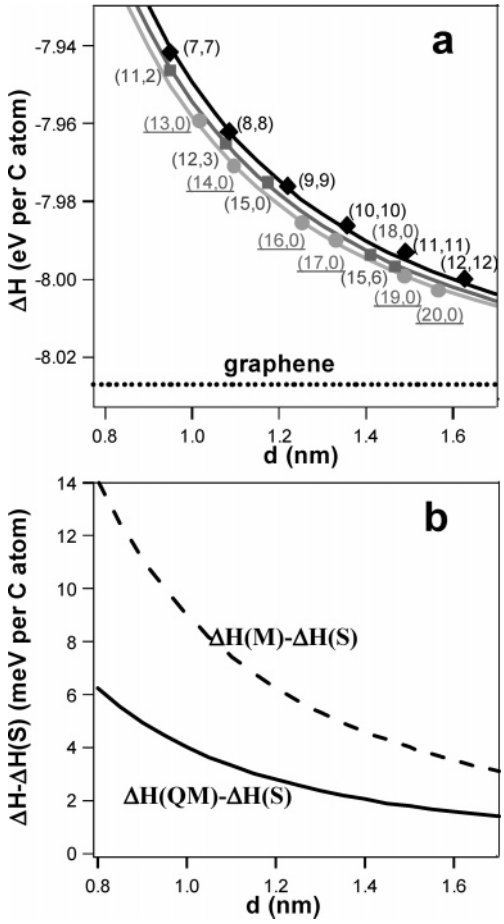

Figure 4. (a) Density functional theory (DFT) calculations of the atomic heat of formation (ΔH) versus tube diameter (d) for various M-, QM-, and S-SWNTs (denoted by symbols); the three solid lines are $\sim 1/d^2$ fits for the formation energy, relative to graphene, for the three types of tubes. (b) Difference in formation energies between M- and S-SWNTs (dashed line) and QM- and S-SWNTs (solid line), versus tube diameter d; note that, for a SWNT with $d \approx 1$ nm, although the per atom energy gain for a semiconductor is small (a few meV), the energy cost for adding a "belt" of atoms (extending the tube length by one C−C bond length) for the S-SWNT is lower than that for a M-SWNT (by ∼0.15 eV), which is quite substantial ($k_BT \approx 0.07$ eV at 600 °C). This energy is relevant, because SWNT growth from a seed particle occurs via supersaturation and precipitation of C atoms around the particle circumference.

exhibit lower formation energies than QM-SWNTs (by ∼4 meV/d^2; see solid line in Figure 4b) and then M-SWNTs (by ∼9 meV/d^2; see dashed line in Figure 4b).

The $\Delta H - \Delta H$(graphene) $\approx 1/d^2$ fits in Figure 4a are in agreement with theoretical calculations performed previously[16−18] and are mainly due to strain energies in the tubes that are absent in a flat graphene. The discernible differences in the formation energies for metallic, quasi-metallic, and semiconducting SWNTs are revealed here for the first time: earlier calculations have mainly elucidated the diameter dependence but not the dependence on the chirality or metallicity. It is reasonable that, for similar diameters, S-SWNTs are lower in energy than metallic tubes, because of the electronic energy gain that results from the band gap opening in the former. A relevant topic is that the driving force for Peierls instability in a one-dimensional (1D) metal is the band gap opening for reducing the electronic energy of the system. Metallic quasi-1D SWNTs do exist, because they are stable against Peierls distortion over a wide range of temperatures, because of the high cost in lattice distortion energy.[19] Nevertheless, M-SWNTs do exhibit higher electronic energies than semiconducting tubes with similar diameter.

The lower energy of S-SWNTs than M-/QM-SWNTs is more appreciable for nanotubes with smaller diameters than larger nanotubes, because of the $\sim 1/d^2$ dependence (see Figure 4). This theoretical result may be related to the preferential formation of semiconducting nanotubes (for tubes with $d \approx 1.1$ nm) and suggests that the energies and thermodynamics associated with the various nanotube structures could be a factor in determining the types of nanotubes that are grown. The relatively low temperature used in our SWNT synthesis may allow for a clear manifestation of the preferential growth effect. We did vary the PECVD growth temperature from 600 °C to 750 °C and observed no drastic differences in the diameter distribution and the percentage of S-SWNTs for samples grown in this temperature range. For even higher temperatures of 850−900 °C for our typical methane CVD,[14,20] the same catalyst afforded nanotubes with $d = 1.85 \pm 0.55$ nm without any preference in semiconducting tubes (∼60%−70%).

It is instructive to note that, for S- and M-SWNTs with $d \approx 1$ nm, the per-unit-length formation energy is lower for S-SWNTs, by ∼0.15 eV per C−C bond length of 1.46 Å (or a stabilization energy of ∼ 1.0 eV/nm), based on the atomic heats of formation indicated in Figure 4. This is substantial ($k_BT \approx 0.07$ eV at 600 °C) and could be a driving force for the lengthening of nanotubes from the seed catalyst particles[14] preferential into semiconductors. We do note that energetics is a thermodynamic factor that is involved in the growth process. The fact that, at a fixed temperature of 600 °C, increasing the

carbon feedstock by higher plasma power allowed for larger particles, producing larger-diameter SWNTs, suggests the importance of the chemistry in the nanoparticles and kinetic factors involved. Our results here do reveal that, in the temperature range investigated, the small-diameter SWNTs that were produced had a tendency to be rich in semiconductors.

Our theoretical results here are in agreement with the literature reports of higher chemical reactivity for M-SWNTs than S-SWNTs.[21] We also note a recent report of an unexplained high enrichment of S-SWNTs for the nanotube fraction with small diameters (less than ~1 nm) probed by Raman spectroscopy in a separation work with the high-pressure carbon monoxide conversion (HiPCO) material.[7] Such enrichment can be due to the existence of a higher percentage of small-diameter S-SWNTs in the starting as-grown material. Another related phenomenon is that the percentage of S-SWNTs in as-grown HiPCO material (average tube diameter of $d \approx 1-1.1$ nm) has been determined to be significantly higher than that in laser ablation material (average tube diameter of $d \approx 1.5$ nm).[11] All of these results suggest the generality of the enrichment of small-diameter semiconducting SWNTs synthesized by various methods. For the same synthesis method, smaller tubes could be more likely than larger tubes to become semiconductors. Overall, we suggest that diameter control will be a key to the ultimate metallicity control of synthesized nanotubes.

References and Notes

(1) Dresselhaus, M. S.; Dresselhaus, G.; Eklund, P. C. *Science of Fullerenes and Carbon Nanotubes*; Academic Press: San Diego, CA, 1996.

(2) Tans, S.; Verschueren, A.; Dekker, C. *Nature* **1998**, *393*, 49.

(3) Javey, A.; Guo, J.; Wang, Q.; Lundstrom, M.; Dai, H. *Nature* **2003**, *424*, 654.

(4) Kong, J.; Franklin, N. R.; Zhou, C.; Chapline, M. G.; Peng, S.; Cho, K.-j.; Dai, H.; *Science* **2000**, *287*, 622.

(5) Dai, H. *Surf. Sci.* **2002**, *500*, 218.

(6) Chattopadhyay, D.; Galeska, L.; Papadimitrakopoulos, F. *J. Am. Chem. Soc.* **2003**, *125*, 3370.

(7) Samsonidze, Ge. G.; Chou, S. G.; Santos, A. P.; Brar, V. W.; Dresselhaus, G.; Dresselhaus, M. S.; Selbst, A.; Swan, A. K.; Ünlü, M. S.; Goldberg, B. B.; Chattopadhyay, D.; Kim, S. N.; Papadimitrakopoulos, F. *Appl. Phys. Lett.* **2004**, *85*, 1006.

(8) Krupke, R.; Hennrich, F.; von Löhneysen, H.; Kappes, M. M. *Science* **2003**, *301*, 344.

(9) Chen, Z.; Du, X.; Du, M.-H.;Rancken, C. D.; Cheng, H.-P.; Rinzler, A. G. *Nano Lett.* **2003**, *3*, 1245.

(10) Zheng, M.; Jagota, A.; Semke, E. D.; Diner, B. A.; McLean, R. S.; Lustig, S. R.; Richardson, R. E.; Tassi, N. G. *Nature Mater.* **2003**, *2*, 338.

(11) Li, Y. M.; Mann, D.; Rolandi, M.; Kim, W.; Ural, A.; Hung, S.; Javey, A.; Cao, J.; Wang, D.; Yenilmez, E.; Wang, Q.; Gibbons, J. F.; Nishi, Y.; Dai, H. *Nano Lett.* **2004**, *4*, 317.

(12) Bachilo, S. M.; Balzano, L.; Herrera, J. E.; Pompeo, F.; Resasco, D. E.; Weisman, R. B. *J. Am. Chem. Soc.* **2003**, *125*, 11186.

(13) Zhou, C.; Kong, J.; Dai, H. *Phys. Rev. Lett.* **2000**, *84*, 5604.

(14) Li, Y.; Kim, W.; Zhang, Y.; Rolandi, M.; Wang, D.; Dai, H. *J. Phys. Chem. B* **2001**, *105*, 11424.

(15) Kresse, G.; Hafner, J. *Phys. Rev. B* **1994**, *49*, 14251.

(16) Hernandez, E.; Goze, C.; Bernier, P.; Rubio, A. *Appl. Phys. A* **1999**, *68*, 287.

(17) Barnard, A. S.; Snook, I. K. *J. Chem. Phys.* **2004**, *120*, 3817.

(18) Xiao, C.; Chan, H. S. O.; Xu, G. Q.; Lim, K. T.; Lin, J. *Appl. Phys. Lett.* **2004**, *84*, 1677.

(19) Mintmire, J. W.; Dunlap, B. I.; White, C. T. *Phys. Rev. Lett.* **1992**, *68*, 631.

(20) Kong, J.; Soh, H. T; Cassell, A. M.; Quate, C. F.; Dai, H. *Nature* **1998**, *395*, 878.

(21) Strano, M. S.; Dyke, C. A.; Usrey, M. L.; Barone, P. W.; Allen, M. J.; Shan, H.; Kittrell, C.; Hauge, R. H.; Tour, J. M.; Smalley, R. E. *Science* **2003**, *301*, 1519.